Mechanistic Implications from Crystalline Complexes of Wild-Type and Mutant Adenylosuccinate Synthetases from *Escherichia coli*[†,‡]

Jun-Yong Choe, Bradley W. Poland,[§] Herbert J. Fromm, and Richard B. Honzatko*

Department of Biochemistry, Biophysics, and Molecular Biology, Iowa State University, Ames, Iowa 50011

Received January 22, 1999; Revised Manuscript Received April 2, 1999

ABSTRACT: Asp13 and His41 are essential residues of adenylosuccinate synthetase, putatively catalyzing the formation of adenylosuccinate from an intermediate of 6-phosphoryl-IMP. Wild-type adenylosuccinate synthetase and three mutant synthetases (Arg143 → Leu, Lys16 → Gln, and Arg303 → Leu) from *Eschericha coli* have been crystallized in the presence of IMP, hadacidin (an analogue of L-aspartate), Mg^{2+}, and GTP. The active site of each complex contains 6-phosphoryl-IMP, Mg^{2+}, GDP, and hadacidin, except for the Arg303 → Leu mutant, which does not bind hadacidin. In response to the formation of 6-phosphoryl-IMP, Asp13 enters the inner coordination sphere of the active site Mg^{2+}. His41 hydrogen bonds with 6-phosphoryl-IMP, except in the Arg303 → Leu complex, where it remains bound to the guanine nucleotide. Hence, recognition of the active site Mg^{2+} by Asp13 evidently occurs after the formation of 6-phosphoryl-IMP, but recognition of the intermediate by His41 may require the association of L-aspartate with the active site. Structures reported here support a mechanism in which Asp13 and His41 act as the catalytic base and acid, respectively, in the formation of 6-phosphoryl-IMP, and then act together as catalytic acids in the subsequent formation of adenylosuccinate.

Adenylosuccinate synthetase [IMP:L-aspartate ligase (GDP forming), EC 6.3.4.4] is an essential enzyme in *Escherichia coli* and many other forms of life (*1*), catalyzing the first committed step in de novo biosyntheses of AMP:

$$\text{IMP} + \text{L-aspartate} + \text{GTP} \xrightleftharpoons{Mg^{2+}} \text{adenylosuccinate} + \text{GDP} + P_i$$

The catalytic mechanism proceeds with the initial formation of 6-phosphoryl-IMP by nucleophilic attack of the 6-oxo group of IMP on the γ-phosphorus atom of GTP, followed by the nucleophilic displacement of the 6-phosphoryl group by L-aspartate to form adenylosuccinate. Although the sequence of events as specified above enjoys substantial support (*2*−*5*), details regarding the participation of specific side chains in catalysis are, for the most part, conjecture. Asp13 and His41 are both essential to catalysis as demonstrated by directed mutation (*6*). Each side chain putatively catalyzes both steps of the overall reaction (*4*, *5*). Asp13 acts as a catalytic base in the phosphorylation of IMP (proton abstraction from N1 of IMP) and then as a catalytic acid in the nucleophilic displacement of the 6-phosphoryl group (protonation of N1 of 6-phosphoryl-IMP to make C6 more electrophilic). His41 acts as a catalytic acid in the phosphorylation reaction (proton donation to the leaving group, GDP) and again as a catalytic acid in the phosphoryl displacement reaction (proton donation to the phosphate group). On the basis of the proposed catalytic mechanism for the synthetase

Table 1: Statistics of Data Collection and Refinement

	wild-type	Lys16 → Gln	Arg143 → Leu	Arg303 → Leu
resolution (Å)	2.5	2.5	2.5	2.5
no. of measurements	98390	178309	165859	185165
no. of unique reflections	20808	27094	26553	26203
completeness of data				
data set	99	99	99	99
last shell (2.7−2.5 Å)	99	99	99	99
R_{sym}[a]	6.17	7.43	9.08	10.73
no. of reflections in refinement[b]	16481	17691	17987	17525
no. of atoms[c]	4636	4866	4873	4610
no. of solvent sites	200	241	247	174
R-factor[d]	0.160	0.169	0.157	0.179
R_{free}[e]	0.259	0.249	0.240	0.252
mean *B* (Å^2)				
protein	32	18	20	35
6-phosphoryl-IMP	28	15	12	35
GDP	29	20	18	25
hadacidin	35	17	24	−[f]
root-mean-square deviations				
bond lengths (Å)	0.013	0.013	0.012	0.010
bond angles (deg)	1.91	1.97	1.89	1.76

[a] $R_{sym} = \Sigma_j\Sigma_i|I_{ij} - \langle I_j\rangle|/\Sigma_i\Sigma_j I_{ij}$, where *i* runs over multiple observations of the same intensity and *j* runs over crystallographically unique intensities. [b] All data in the resolution range of 5−2.5 Å. [c] Includes hydrogens linked to polar atoms. [d] *R*-factor $= \Sigma||F_{obs}| - |F_{calc}||/\Sigma|F_{obs}|$, where $|F_{obs}| > 0$. [e] *R*-factor based upon 10% of the data randomly culled and not used in the refinement. [f] Hadacidin not bound.

[†] This research was supported in part by Grant NS 10546 from the National Institutes of Health, the U.S. Public Health Service, Grant MCB-9603595 from the National Science Foundation, and Grant 95-37500-1926 from the United States Department of Agriculture. This is journal paper J18262 of the Iowa Agriculture and Home Economics Experiment Station, Ames, IA, Project 3191, and supported by Hatch Act and State of Iowa funds.

[‡] Coordinates and structure factors for the structures described in this paper have been deposited with the Brookhaven Protein Data Bank (file names 1cg0, 1cg1, 1cg3, and 1cg4).

* To whom correspondence should be addressed: Department of Biochemistry and Biophysics, Iowa State University, Ames, IA 50011. Phone: (515) 294-6116. Fax: (515) 294-0453. E-mail: honzatko@iastate.edu.

[§] Present address: Howard Hughes Medical Institute, Baylor College of Medicine, Houston, TX 77030.

10.1021/bi990159s CCC: $18.00
Published on Web 05/06/1999

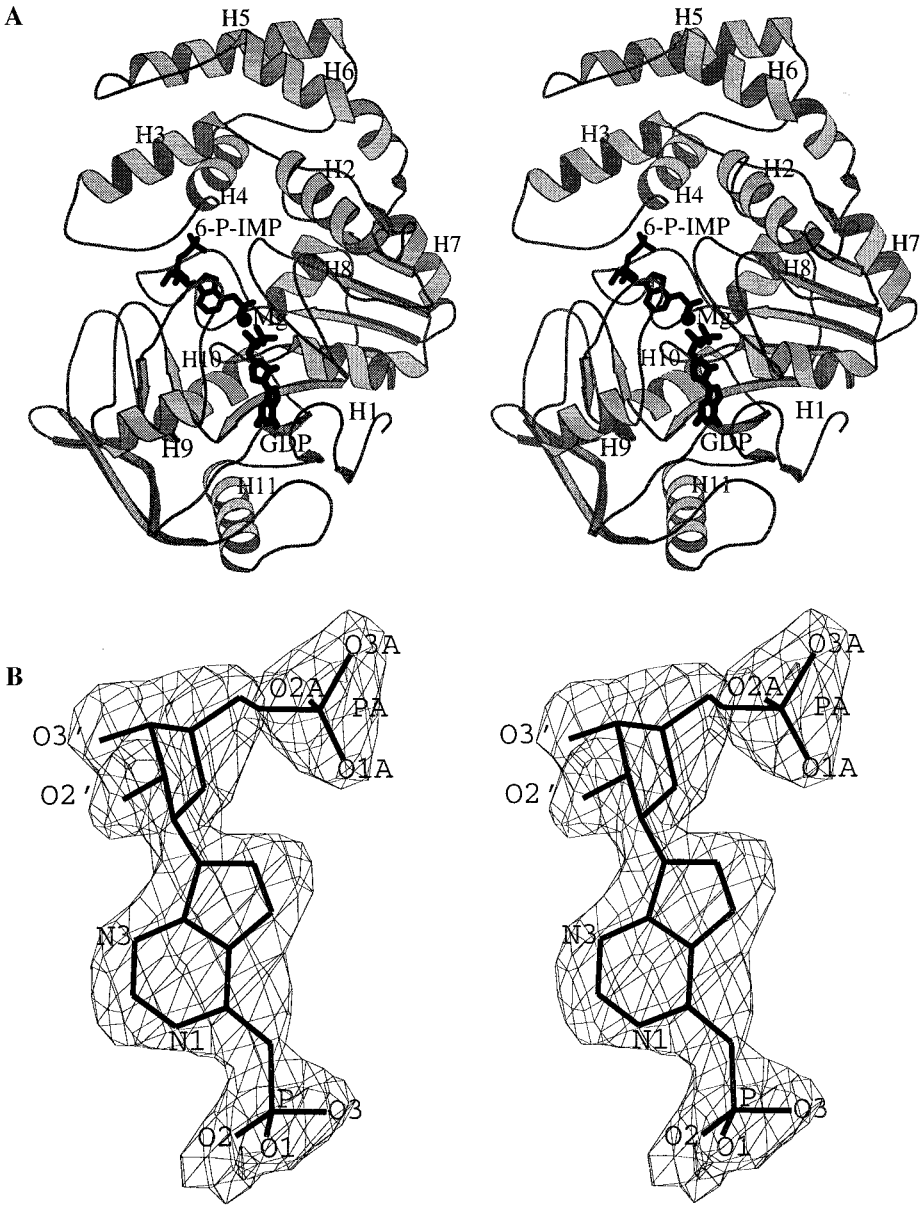

FIGURE 1: Overview of the 6-phosphoryl-IMP complex of the synthetase. (A) A single monomer of the synthetase dimer, drawn with MOLSCRIPT (*24*), showing ligands as ball-and-stick models. Hadacidin is omitted for clarity. (B) Electron density from an omit map of the wild-type complex, contoured at a level of 3σ with a cutoff radius of 1 Å covering the model for 6-phosphoryl-IMP.

(*4*, *5*), the interactions of Asp13 and His41 should differ in synthetase complexes prior to and after the formation of 6-phosphoryl-IMP.

Reported here are crystal structures of wild-type and mutant forms of adenylosuccinate synthetase from *E. coli*. The mutant enzymes, Arg143 → Leu, Lys16 → Gln, and Arg303 → Leu, exhibit k_{cat} parameters that are 100, 50, and 13%, respectively, of that of the wild-type enzyme (*6*−*8*). The crystals were grown in the presence of IMP, GTP, Mg^{2+}, and hadacidin [a competitive inhibitor of L-aspartate (*1*)], but at each active site, electron density is clearly present for 6-phosphoryl-IMP. The above examples represent the first instances of 6-phosphoryl-IMP complexes, and complement structures involving 6-thiophosphoryl-IMP (*5*) and IMP−NO_3^- (*4*). In the presence of 6-phosphoryl-IMP, Asp13 has become an inner sphere ligand of the active site Mg^{2+}. The Mg^{2+} is octahedrally coordinated, as opposed to its square pyramidal coordination in the IMP−NO_3^- complex. Furthermore, in the Arg303 → Leu complex, which does not bind hadacidin, His41 does not hydrogen bond with 6-phosphoryl-IMP. Hence, recognition of the 6-phosphoryl group of the intermediate by His41 may require the association of L-aspartate (or an appropriate analogue) with the active site. The structures presented here support multiple roles for Asp13 and His41 in the proposed catalytic mechanism of the synthetase.

MATERIALS AND METHODS

Purification and Crystallization of the Enzyme from E. coli. Hadacidin was a generous gift from F. Rudolph and B. Cooper (Department of Biochemistry and Cell Biology, Rice University, Houston, TX). All other reagents came from Sigma. The synthetases were prepared as described previously from a genetically engineered strain of *E. coli*, which does not express wild-type adenylosuccinate synthetase from its own genome (*4*, *5*, *9*). The enzymes were at least 95% pure on the basis of SDS−PAGE (data not shown).

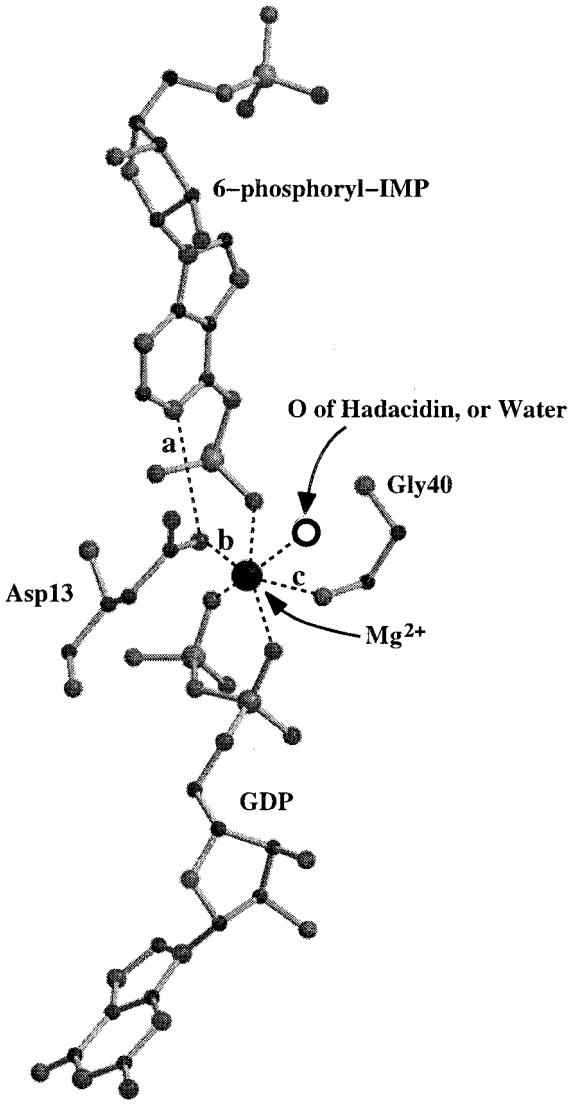

FIGURE 2: Coordination of the active site Mg^{2+}. The letters a−c represent distances in angstroms; for the wild-type, Arg143 → Leu, Lys16 → Gln, and Arg303 → Leu complexes, *a*, *b*, and *c* = 3.2, 2.1, and 2.2 Å, 3.0, 2.3, and 2.1 Å, 3.0, 2.4, and 2.1 Å, and 3.0, 2.6, and 1.9 Å, respectively. The open circle represents the position of a coordinated oxygen atom from either the *N*-formyl group of hadacidin (wild-type, Arg143 → Leu, and Lys16 → Gln complexes) or water (Arg303 → Leu complex).

Crystals were grown by the method of hanging drops under conditions similar to those employed in previous work (*4*). Droplets contained 2 μL of an enzyme solution [50 mM imidazole, 75 mM succinate, 4 mM GTP, 4 mM IMP, 5 mM hadacidin, and 10 mg/mL protein (pH 7.0)] and 2 μL of a crystallization buffer [13% (w/w) polyethylene glycol 8000, 100 mM cacodylic acid/cacodylate (pH 6.5), and 200 mM magnesium chloride]. The wells contained 500 μL of the crystallization buffer. Crystals of the wild-type, Lys16 → Gln, and Arg143 → Leu enzymes grew in about 1 week to approximately 0.6 mm in all dimensions and belonged to space group $P3_221$ ($a = b = 79.86$ Å and $c = 158.43$ Å at 100 K for the wild-type enzyme, $a = b = 80.37$ Å and $c = 158.52$ Å at 100 K for the Lys16 → Gln enzyme, and $a = b = 80.94$ Å and $c = 158.17$ Å at 100 K for the Arg143 → Leu enzyme). Crystals of the Arg303 → Leu enzyme were smaller (approximately 0.4 mm in all dimensions), belonging also to space group $P3_221$ ($a = b = 80.24$ Å and $c = 157.87$ Å at 100 K). Prior to data collection, crystals were transferred to a freshly prepared solution containing 25% (v/v) glycerol and equal parts of the above protein solution (without the protein) and the crystallization buffer. Glycerol inhibits formation of ice within crystals of the synthetase at temperatures used in data acquisition (approximately 100 K).

Table 2: Selected Contacts Involving Ligand Atoms in 6-Phosphoryl-IMP Complexes of Adenylosuccinate Synthetase

		distance (Å)			
ligand atom	contact atom	wild-type	Lys16 → Gln	Arg143 → Leu	Arg303 → Leu
GDP O1A	Thr42 OG1	3.01	2.89	2.91	3.62
GDP O2A	Arg305 NH2	3.11	2.81	2.91	3.78
GDP O1B	His41 ND1	4.57	4.47	4.63	2.76
6-P-IMP[a] O3	His41 NE2	2.74	2.54	2.62	4.17

[a] 6-Phosphoryl-IMP.

Data Collection. Data from single crystals of each complex were collected at 100 K on a Siemens area detector, using CuKα radiation and a graphite monochromator, and were reduced with XENGEN (*10*). The data sets were 99% complete to at least 2.5 Å for each of the complexes. Crystals of the Arg303 → Leu mutant were smaller and exhibited poorer diffraction than the other synthetase complexes reported here (Table 1).

Model Refinement. Starting phases were calculated from the GDP complex (*4*), omitting all ligands and solvent. Refinement procedures are as described previously (*4*), except here an overall anisotropic scale factor was employed. The ligand models were fit to omit electron density maps, followed by a cycle of refinement using XPLOR (*11*). Constants of force and geometry for the protein came from Engh and Huber (*12*) and those for hadacidin from Poland et al. (*4*). In early rounds of refinement, models were heated to 2000 K and then cooled in steps of 25−300 K. In later rounds of the refinement, the systems were heated to 1000 or 1500 K and cooled in steps of 10 K. After the slow cooling protocol was complete (at 300 K), the models were subjected to 120 steps of conjugated gradient minimization, followed by 20 steps of individual *B*-parameter refinement. Individual *B*-parameters were subject to the following restraints: nearest neighbor, main chain atoms, 1.5 Å^2; next-to-nearest neighbor, side chain atoms, 2.0 Å^2; nearest neighbor, side chain atoms, 2.0 Å^2; and next-to-nearest neighbor, side chain atoms, 2.5 Å^2. Criteria for the addition of water molecules were identical to those of previous studies (*4*, *5*).

RESULTS

Quality of the Refined Models. The method of Luzzati (*13*) indicates an uncertainty in coordinates of 0.30 Å. The amino acid sequence used in refinement is identical to that reported previously (*14*, *15*). Results of data collection and refinement are listed in Table 1. An overview of the 6-phosphoryl-IMP complex and an image of the 6-phosphoryl intermediate covered by electron density from the wild-type structure are shown in Figure 1. Gln10 is the only serious violation of the Ramachandran plot as identified by PROCHECK (*16*). The conformation of Gln10 is enforced by its hydrogen bonding environment as described previously (*14*, *15*). The models have better stereochemistry than is typical for structures based upon data of comparable resolution. Thermal

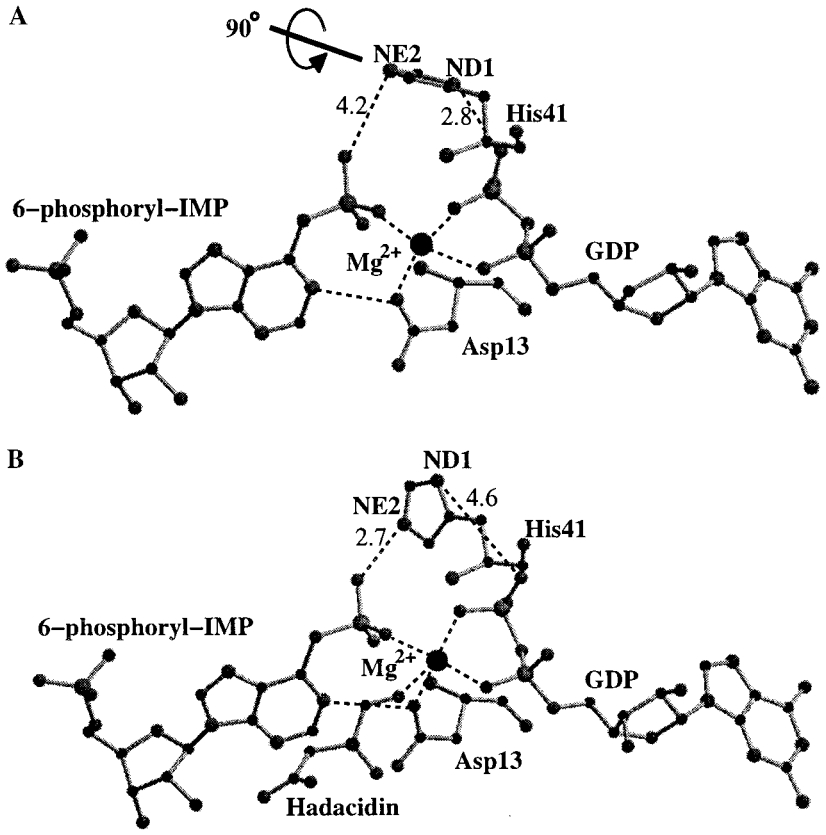

FIGURE 3: Two conformational states of His41. Interactions of His41 in the Arg303 → Leu complex (A) and the wild-type complex (B). Distances in angstroms, associated with dashed lines, are measured from atoms ND1 and NE2 of His41 to oxygen atoms of the 6-phosphoryl group of 6-phosphoryl-IMP and the β-phosphoryl group of GDP.

parameters vary in the complexes from 7 to 70, 5 to 65, 5 to 50, and 8 to 89 Å^2 for the wild-type, Arg143 → Leu, Lys16 → Gln, and Arg303 → Leu complexes, respectively. The variation in thermal parameters as a function of residue is comparable to that of other structures of the ligated synthetase (*4*, *5*). Data from crystals of the Arg303 → Leu complex exhibit anisotropy as inferred by a significant reduction (approximately 0.05) in R_{free} when an overall anisotropic scale factor was used to scale calculated and observed structure factors. The anisotropy for data collected from the Arg303 → Leu crystal is probably a consequence of its inability to bind hadacidin, as even crystals of the wild-type enzyme, grown without hadacidin, exhibit the same phenomenon (Z. Hou and R. B. Honzatko, unpublished). Furthermore, data sets from crystals of the wild-type complex and of the other mutants reported here bind hadacidin and do not exhibit significant anisotropy. Thermal parameters for individual ligands average to less than 35 Å^2 in all complexes. Pairwise superposition of the structures results in root-mean-square deviations in Cα coordinates of 0.3 Å, comparable to the estimate of coordinate uncertainty.

The 6-phosphoryl-IMP complexes are similar in conformation to the IMP−NO_3^- complex (*4*) and the 6-thiophosphoryl-IMP complex (*5*). Hence, to avoid redundancy here, the focus will be on significant conformational differences between the 6-phosphoryl-IMP complexes and previously published complexes of the synthetase.

Mg^{2+} Coordination. In the wild-type and mutant 6-phosphoryl-IMP complexes, bound Mg^{2+} is octahedrally coordinated (Figure 2). Oxygen atoms from the α- and β-phosphoryl groups of GDP, from the 6-phosphoryl group of the intermediate, from the *N*-formyl group of hadacidin (a water molecule in the case of the Arg303 → Leu mutant complex), from backbone carbonyl 40, and from Asp13 are all within 2.7 Å of the metal cation. In contrast, coordination of bound Mg^{2+} is square pyramidal in the IMP−NO_3^- complex (*4*) and the 6-thiophosphoryl-IMP complex (*5*), the aberrant distance involving atom OD1 of Asp13. The distance of separation between OD1 of Asp13 and Mg^{2+} in the wild-type, Lys16 → Gln, and Arg143 → Leu complexes averages to 2.25 Å as opposed to an average value of 3.05 Å for the IMP−NO_3^- and 6-thiophosphoryl-IMP complexes. The difference in the two measures (0.8 Å) is more than double the level of coordinate uncertainty.

Unfortunately, the potential energy field used in refinement will introduce systematic errors in the structure. The most serious artifact in ligated structures of the synthetase comes from electrostatic interactions. In the case of the IMP−NO_3^- complex (*4*), for instance, the refined distance between OD1 of Asp13 and the metal cation is 2.7 Å, using the standard set of electrostatic charges on individual atoms. In such refinements, the side chain of Asp13 is noticeably out of its electron density, being drawn toward the metal cation (B. W. Poland and R. B. Honzatko, unpublished). Scaling electrostatic charges by a factor of 0.25 and the elimination of charge on the cation, however, allow the electron density to determine the position of the side chain of Asp13 relative to the metal cation. Inner sphere coordinate bonds to the Mg^{2+} are insensitive to the scaling of electrostatic charges and/or the elimination of charge assigned to the cation. The average coordination distance for inner sphere ligands, using a metal cation with a charge of zero, is 2.14 Å, whereas for

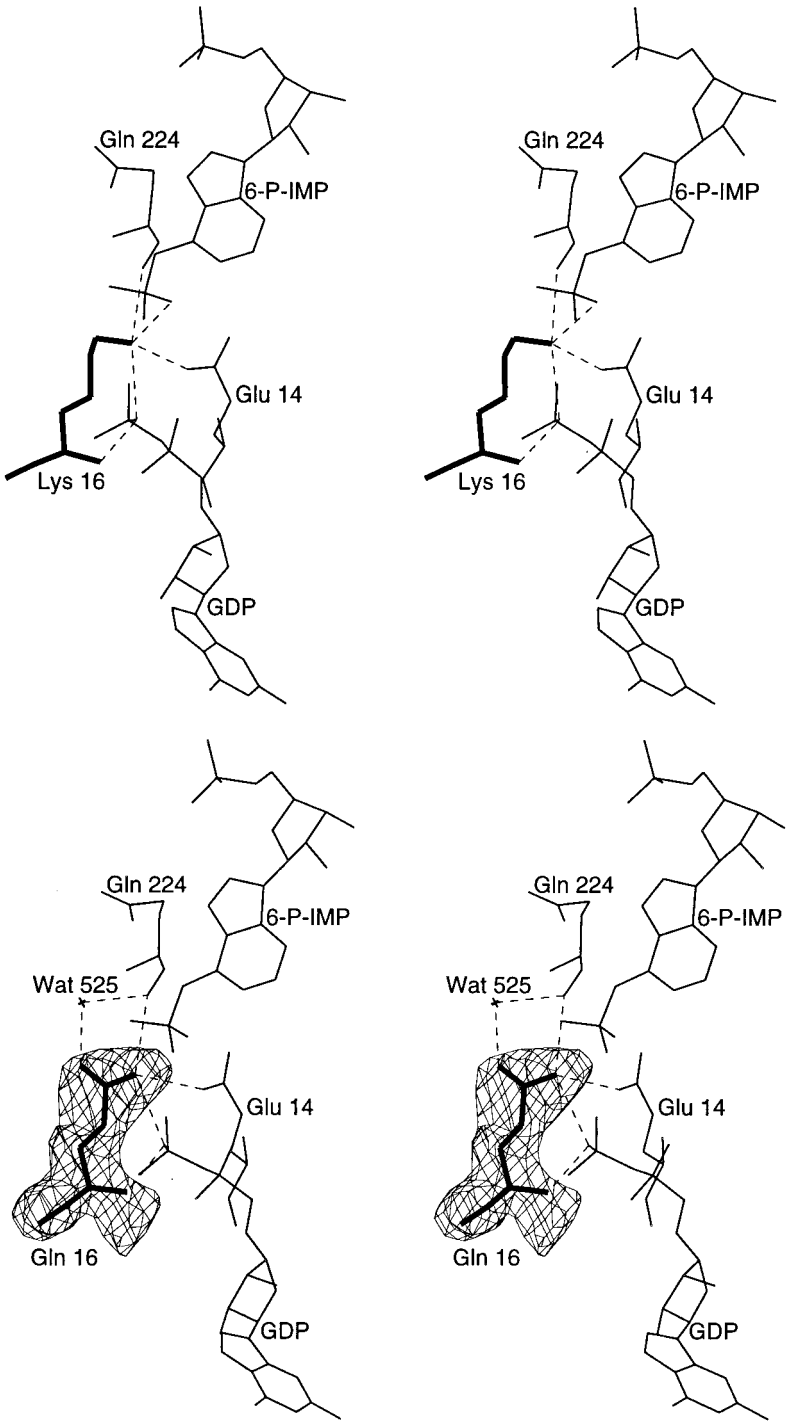

FIGURE 4: Stereoview of wild-type and Lys16 → Gln complexes in the vicinity of the 6-phosphoryl binding pocket. Electron density for the side chain of Gln16 contoured at 3σ, using a cutoff radius of 1 Å. Dashed lines represent donor−acceptor interactions, and bold lines represent the residue at position 16.

a metal cation with a charge of 0.5, the average becomes 2.11 Å. Repulsive van der Waals forces between the coordinating oxygen atoms and the metal cation prevent significant shortening of the inner sphere coordinate bonds as partial electrostatic charges are scaled up to their full values. Evidently, the force field bias reduces the distance between OD1 of Asp13 and the Mg^{2+} in synthetase complexes which exhibit square pyramidal coordination of the metal cation, but has little influence on distances involving inner sphere atoms. The 0.8 Å movement of OD1 of Asp13 toward Mg^{2+} then may be a conservative estimate of the conformational relaxation of Asp13 in response to the formation of the 6-phosphoryl intermediate.

α-*Phosphoryl Site of GDP*. In the wild-type, Lys16 → Gln, and Arg143 → Leu complexes, the side chains of Arg305 and Thr42 hydrogen bond with the α-phosphoryl group of GDP. Both of these hydrogen bonds are absent, however, in the Arg303 → Leu complex (Table 2). The loss of these hydrogen bonds and the conformational change in the side chain of His41 (see below) are correlated with the absence of bound hadacidin in the L-aspartate pocket.

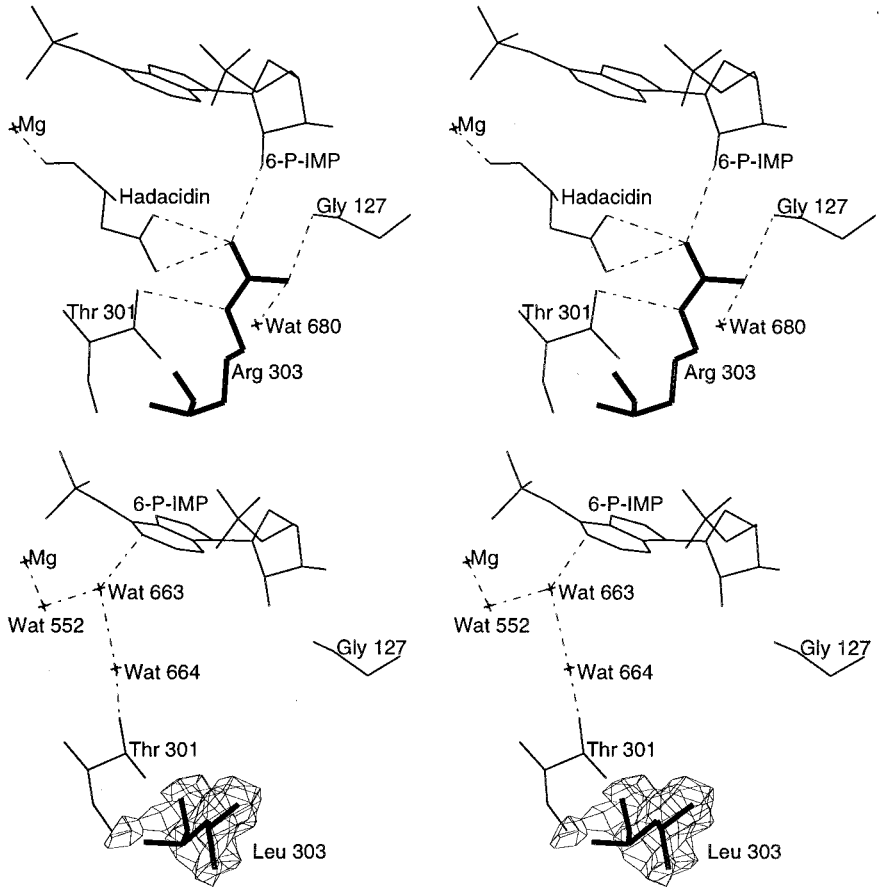

FIGURE 5: Stereoview of wild-type and Arg303 → Leu complexes in the vicinity of the L-aspartate binding site. Electron density for the side chain of Leu303 contoured at 3σ, using a cutoff radius of 1 Å. Dashed lines represent donor−acceptor interactions, and bold lines represent the residue at position 303.

γ-Phosphoryl or 6-Phosphoryl Site. NE2 of His41 hydrogen bonds with the 6-phosphoryl group of the intermediate in the wild-type, Lys16 → Gln, and Arg143 → Leu complexes (donor−acceptor distance of approximately 2.6 Å; Table 2). In the Arg303 → Leu complex, His41 does not hydrogen bond with the 6-phosphoryl group (the corresponding distance is 4.2 Å). In fact, His41 in the Arg303 → Leu complex hydrogen bonds with the β-phosphoryl group of GDP (Figure 3). In the IMP−NO_3^- complex (*4*), His41 hydrogen bonds with the β-phosphoryl group of GDP, whereas in the 6-thiophosphoryl-IMP complex (*5*), it hydrogen bonds with the 6-thiophosphoryl group. In past work, the two conformations of His41 were attributed to differences in electrostatic charge of the nitrate anion and the 6-thiophosphoryl group (*5*). In the series of structures reported here, however, the 6-phosphoryl group is present at each active site. Hence, other factors must influence the conformation of His41. As discussed below, the interaction of hadacidin at the L-aspartate pocket could stabilize the hydrogen bond between His41 and the 6-phosphoryl group.

Lys16 hydrogen bonds with the 6-phosphoryl group of the intermediate and (perhaps more weakly) with the β-phosphoryl group of GDP (Figure 4). The substitution of glutamine for lysine at position 16 has only minor effects on the structure. The relative positions of NE2 of Gln16 and NZ of Lys16 are nearly the same. Donor−acceptor distances from NE2 of Gln16 to the 6-phosphoryl group, the β-phosphoryl group of GDP, and the side chain of Glu14 are 3.6, 3.2, and 3.0 Å, respectively. The corresponding distances for NZ of Lys16 are approximately 3.0, 3.0, and 3.1 Å, respectively. OE1 of Gln16, however, makes a close nonbonded contact (2.9 Å) with backbone carbonyl 222. In the wild-type enzyme, backbone carbonyl 222 makes a more favorable nonbonded contact (3.4 Å) with CE of Lys16.

L-*Aspartate Binding Pocket*. Hadacidin does not bind to the putative L-aspartate pocket in the Arg303 → Leu complex (Figure 5). Instead, three water molecules fill the void normally occupied by hadacidin. One water molecule (Wat552) is in the inner sphere of the active site Mg^{2+}. A second water molecule (Wat664) hydrogen bonds to Thr301 and, in concert with the Mg^{2+}-coordinated water molecule, stabilizes a third water molecule (Wat663) in van der Waals contact with N1 and C6 of 6-phosphoryl-IMP.

5′-Phosphoryl Site of the Inosine Nucleotide. The mutation of Arg143 to leucine removes the direct interaction of the guanidinium group with the 5′-phosphoryl group of the inosine nucleotide. Bound water molecules, however, structurally compensate for the lost guanidinium group (Figure 6). One water molecule (Wat697) hydrogen bonds backbone carbonyl 238 and an oxygen of the 5′-phosphoryl group, and a second water molecule (Wat773) hydrogen bonds with two additonal water molecules. The two waters, named above, are structural analogues of the NH_2 groups of Arg143.

DISCUSSION

On the basis of this and previous work (*4*−*6*), either ND1 of His41 can hydrogen bond with the β-phosphoryl group

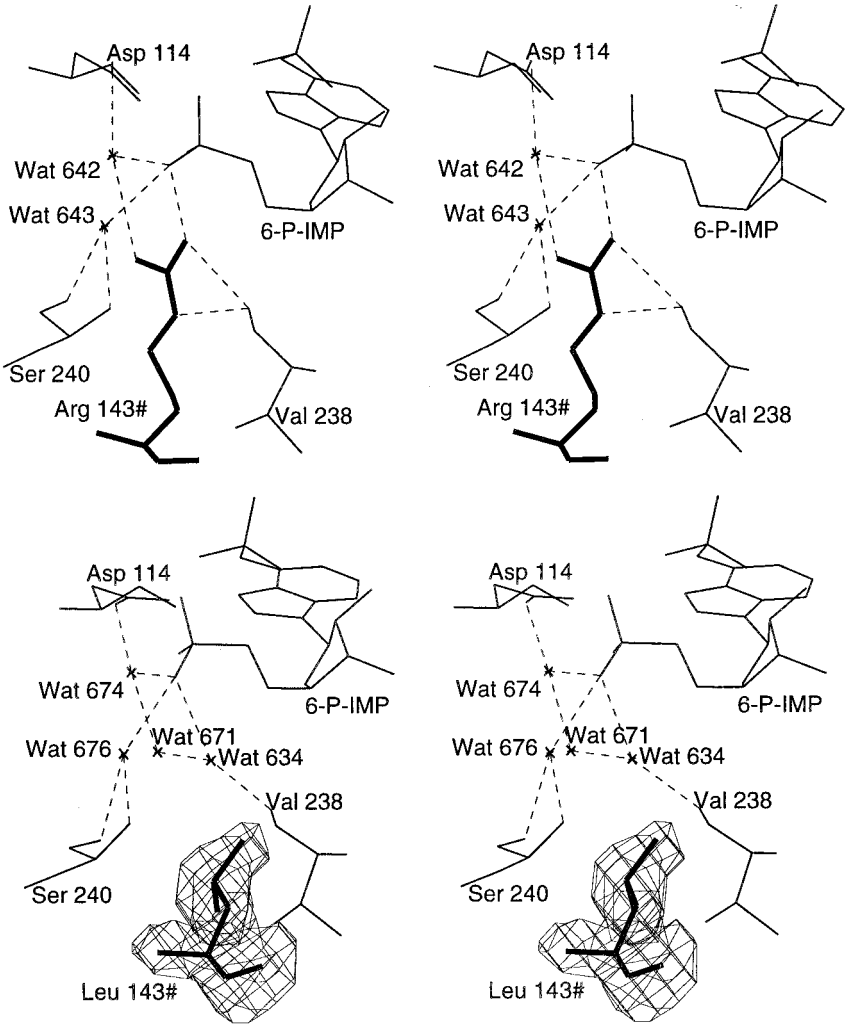

FIGURE 6: Stereoview of wild-type and the Arg143 → Leu complexes in the vicinity of the IMP binding site. Electron density for the side chain of Leu143 contoured at 3σ, using a cutoff radius of 1 Å. Dashed lines represent donor−acceptor interactions, and bold lines represent the residue at position 143 of the subunit related by molecular 2-fold symmetry.

of the guanine nucleotide or NE2 of His41 can hydrogen bond with the 6-phosphoryl group of the intermediate. The side chain of His41 must undergo a rotation of approximately 90° about its Cβ−Cγ bond in crossing from one state of hydrogen bonding to the other. The structural data are consistent with two possible roles for His41 in the phosphotransfer reaction. (i) His41 binds to the β-phosphoryl group of GTP and donates a proton to the leaving group. (ii) His41 binds to the γ-phosphoryl group of GTP, enhancing the electrophilic character of Pγ by polarizing a P−O bond. On the basis of the IMP−NO_3^- complex (*4*), which putatively represents the transition state of the phosphotransfer reaction, His41 hydrogen bonds with the β-phosphoryl group of GDP. Largely because of this structure, we favor the first of the above mechanistic alternatives, in which His41 acts as an acid catalyst during the phosphotransfer reaction (Figure 7). After the protonation of the leaving group (GDP), His41 must dissociate from bound GDP, become reprotonated, and undergo the 90° rotation about its Cβ−Cγ bond, before it hydrogen bonds with the 6-phosphoryl group of the intermediate.

As His41 binds to the β-phosphoryl group of GDP and not to the 6-phosphoryl group of the intermediate in the Arg303 → Leu complex, ligation of the L-aspartate pocket may be a prerequisite for the recognition of the 6-phosphoryl group by His41. Such a mechanism would ensure against full activation of the 6-phosphoryl group until L-aspartate is positioned properly. Furthermore, the putative coupling between His41 and the L-asparate pocket is supported by other conformational differences, as well as by changes in kinetics due to point mutations. Hydrogen bonds involving the side chains of Thr42 and Arg305 with the α-phosphoryl group of the guanine nucleotide are absent in the Arg303 → Leu complex, but are clearly present in the other complexes which have a ligated L-aspartate pocket (Table 2). The mutation of His41 to asparagine has little effect on the K_m of IMP, but increases the K_m of L-aspartate and GTP by 9- and 5-fold, respectively (Table 3). Evidently, the ligation of the L-aspartate pocket by hadacidin goes beyond stabilization of the 300s loop (residues 299−304) to include subtle effects at the guanine nucleotide pocket. Hadacidin [and also probably L-aspartate (*4*)] interacts directly with Arg305, and in so doing may stabilize hydrogen bonds involving the side chains of Thr42 and Arg305 with GDP. Hence, Mg^{2+} and Arg305 evidently work in concert to draw hadacidin and GDP together in a tight complex, the formation of which favors the interaction between His41 and the 6-phosphoryl group of the intermediate.

Asp13 may be the most important catalytic residue of the synthetase. The mutation of Asp13 to alanine abolishes

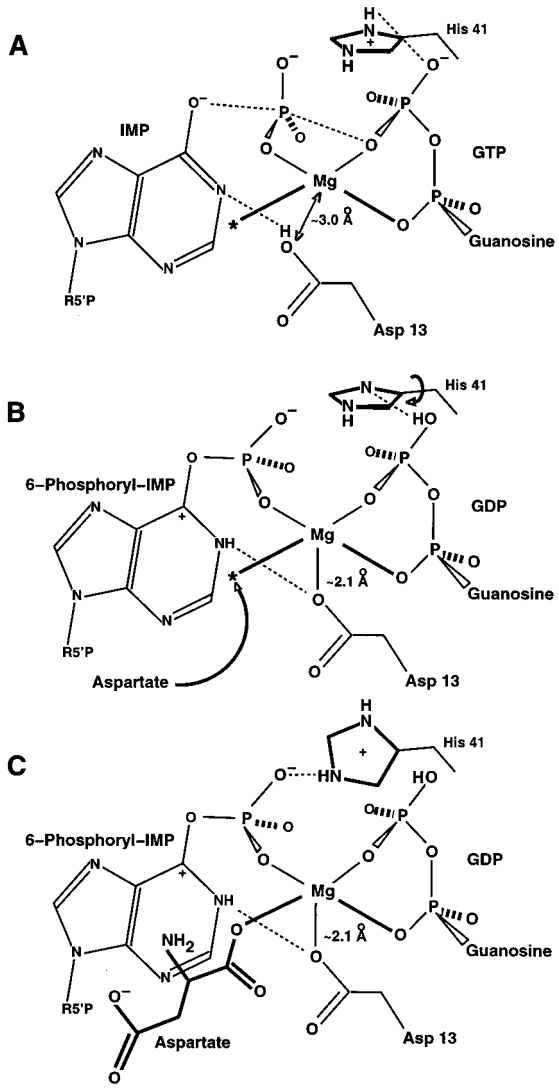

FIGURE 7: Schematic representation of suggested conformational responses in Asp13 and His41. Interactions that are probably significant to catalysis are represented by dashed lines. The coordination of backbone carbonyl 40 with the active site Mg^{2+} is omitted for clarity. (A) Transition state for the phosphotransfer reaction in which Asp13 acts as a catalytic base (proton abstraction from N1 of IMP) and His41 acts as a catalytic acid (protonation of GDP). The asterisk represents the coordination site for L-aspartate, which need not be present for the first reaction. (B) 6-Phosphoryl-IMP complex prior to the association of L-aspartate. Asp13 has become a ligand of the active site Mg^{2+}. (C) 6-Phosphoryl-IMP complex with bound L-aspartate. The conformational change in His41 is putatively triggered by the association of L-aspartate.

Table 3: Kinetic Parameters for Wild-Type and Mutant Forms of Adenylosuccinate Synthetase

protein (ref)	k_{cat} (s^{-1})	$K_{m,GTP}$ (μM)	$K_{m,IMP}$ (μM)	$K_{m,aspartate}$ (mM)
wild-type (*7*)	1.00 ± 0.005	26 ± 2	28 ± 1	0.23 ± 0.04
His41 → Asn (*6*)	0.0095 ± 0.0001	130 ± 10	40 ± 8	2.0 ± 0.6
Arg143 → Leu (*8*)	1.01 ± 0.01	280 ± 30	2800 ± 100	0.34 ± 0.06
Lys16 → Gln (*6*)	0.5 ± 0.1	23 ± 7	50 ± 20	0.31 ± 0.06
Arg303 → Leu (*7*)	0.13 ± 0.01	20 ± 1	35 ± 4	57 ± 7

measurable activity (*6*). In the IMP, NO_3^-, GDP, and hadacidin complex (*4*), Asp13 hydrogen bonds with N1 of IMP, but does not coordinate with Mg^{2+}. The above observations are consistent with Asp13 acting as a catalytic base, abstracting the proton from N1 of IMP (*4*−*6*). Poland et al. (*4*) suggest that the formation of 6-phosphoryl-IMP could alter the environment of the active site so as to permit the coordination of Asp13 to Mg^{2+}. The coordination of protonated Asp13 to Mg^{2+} necessarily transforms the side chain into a potent catalytic acid. The proton, abstracted by Asp13 in the phosphotransfer step, then, is forced back onto N1 of the intermediate, increasing the electrophilic character of C6 (Figure 7). Structures of the 6-phosphoryl-IMP complexes presented here support this dual catalytic role for Asp13. To within experimental error, OD1 of Asp13 maintains a hydrogen bond with N1 of the 6-phosphoryl intermediate (Figure 2), while being coordinated to Mg^{2+}.

The presence of 6-phosphoryl-IMP and GDP in each of the active sites indicates that all of these systems can catalyze the phosphotransfer reaction. Indeed, the least active of the synthetases described here (Arg303 → Leu) has a k_{cat} which is still 13% of that of the wild-type enzyme (Table 3). The mutation of Lys16 to glutamine reduces k_{cat} by only 50% relative to that of the wild-type enzyme, and has little effect on K_m parameters for substrates (Table 3). The Lys16 → Gln complex exhibits no significant change in the relative positions of ligands and functional groups of demonstrated importance to catalysis [Asp13, Asp21, Asn38, His41, Gln224, and Mg^{2+} (*2*, *6*, *18*, *19*)]. Lys16 of the synthetase corresponds structurally to the catalytic lysine of G-proteins (*20*, *21*) and the catalytic lysine of adenylate kinase (*22*, *23*). The absence of a large effect on k_{cat} for the mutation of Lys16 may reflect a fundamental difference in the mechanisms of these systems. Alternatively, Lys16 may still play a catalytic role in the first (phosphotransfer) reaction of the synthetase, but not the second (phosphoryl displacement) reaction. The relative rates of the two partial reactions are unknown. Hence, if the second reaction is slow relative to the first, then the effects of subtle mutations at position 16 may be hidden by the rate-limiting step of the overall reaction.

The absence of hadacidin at the L-aspartate pocket of the Arg303 → Leu complex is again fully consistent with the 250-fold increase in the K_m for L-aspartate due to the mutation (Table 3). In an apparent contradiction to the solution properties of the Arg143 → Leu enzyme, however, the IMP pocket is occupied in the crystalline complex, even though the K_m for IMP is reportedly 100-fold higher for this mutant synthetase than for the wild-type enzyme (Table 3). The discrepancy here may stem from the state of the Arg143 → Leu enzyme in solution under conditions of crystallization as opposed to that under conditions of kinetic assay. The Arg143 → Leu enzyme is present in crystallization experiments at concentrations that are 1000-fold higher than those in assays. At concentrations of 20 mg/mL, the Arg143 → Leu synthetase is a dimer, whereas at 20 μg/mL, the enzyme is monomeric (*8*). Hence, under the conditions of assay, the K_m may reflect IMP interactions with synthetase monomers, whereas in crystallization experiments, IMP interacts with preformed synthetase dimers, which in turn are removed from solution by the process of crystallization.

REFERENCES

1. Stayton, M. M., Rudolph, F. B., and Fromm, H. J. (1983) *Curr. Top. Cell. Regul. 22*, 103−141.
2. Lieberman, I. (1956) *J. Biol. Chem. 223*, 327−339.
3. Fromm, H. J. (1958) *Biochim. Biophys. Acta 29*, 255−262.

4. Poland, B. W., Fromm, H. J., and Honzatko, R. B. (1996) *J. Mol. Biol. 264*, 1013−1027.
5. Poland, B. W., Bruns, C., Fromm, H. J., and Honzatko, R. B. (1997) *J. Biol. Chem. 272*, 15200−15205.
6. Kang, C., Sun, N., Poland, B. W., Gorrell, A., Honzatko, R. B., and Fromm, H. J. (1997) *J. Biol. Chem. 272*, 11881−11885.
7. Wang, W., Poland, B. W., Honzatko, R. B., and Fromm, H. J. (1995) *J. Biol. Chem. 270*, 13160−13163.
8. Wang, W., Gorrell, A., Honzatko, R. B., and Fromm, H. J. (1997) *J. Biol. Chem. 272*, 7078−7084.
9. Bass, M. B., Fromm, H. J., and Stayton, M. M. (1987) *Arch. Biochem. Biophys. 256*, 335−342.
10. Howard, A. J., Nielson, C., and Xuong, N. H. (1985) *Methods Enzymol. 114*, 452−472.
11. Brünger, A. T. (1992) *XPLOR, version 3.1. A system for X-ray crystallography and NMR*, Yale University Press, New Haven, CT.
12. Engh, R. A., and Huber, R. (1991) *Acta Crystallogr. A47*, 392−400.
13. Luzzati, V. (1956) *Acta Crystallogr. 5*, 802−810.
14. Poland, B. W., Silva, M. M., Serra, M. A., Cho, Y., Kim, K. H., Harris, E. M. S., and Honzatko, R. B. (1993) *J. Biol. Chem. 268*, 25334−25342.
15. Silva, M. M., Poland, B. W., Hoffman, C. R., Fromm, H. J., and Honzatko, R. B. (1995) *J. Mol. Biol. 254*, 431−446.
16. Laskowski, R. A., MacArthur, M. W., Moss, D. S., and Thorton, J. M. (1993) *J. Appl. Crystallogr. 26*, 283−291.
17. Bass, M. B., Fromm, H. J., and Rudolph, F. B. (1984) *J. Biol. Chem. 259*, 12330−12333.
18. Wang, W., Hou, Z., Honzatko, R. B., and Fromm, H. J. (1997) *J. Biol. Chem. 272*, 16911−16916.
19. Wang, W., Gorrell, A., Hou, Z., Honzatko, R. B., and Fromm, H. J. (1998) *J. Biol. Chem. 273*, 16000−16004.
20. Saraste, M., Sibbald, P. R., and Wittinghofer, A. (1990) *Trends Biochem. Sci. 15*, 430−434.
21. Segel, I. S., Gibbs, J. B., D'Alonzo, J. S., Temeles, G. L., Wolanski, B. S., Socher, S. H., and Scolnick, E. M. (1986) *Proc. Natl. Acad. Sci. U.S.A. 83*, 952−956.
22. Reinstein, J., Schlichting, I., and Wittinghofer, A. (1990) *Biochemistry 29*, 7451−7459.
23. Tian, G., Yan, H., Jiang, R., Kishi, F., Nakazawa, A., and Tsai, M. (1990) *Biochemistry 29*, 4296−4304.
24. Kraulis, J. (1991) *J. Appl. Crystallogr. 24*, 946−950.

BI990159S